

Electrostatic Influence on Ion Transport through the α HL Channel

M. Misakian, J.J. Kasianowicz

National Institute of Standards and Technology, Biotechnology Division, ACSL 227/A251, Gaithersburg, MD 20899-8313, USA

Received: 21 January 2003/Revised: 10 July 2003

Abstract. The current-voltage relationship of a single *Staphylococcus aureus* α -hemolysin (α HL) channel is nonlinear, rectifying, and depends on the bulk pH and the ionic strength. The data are described qualitatively by a simple one-dimensional Nernst-Planck analysis in which the fixed charges inside and near the pore's entrances affect the transport of ions through the channel. The distances of these fixed charges from one of the channel's entrances are obtained from the channel's crystal structure. The model demonstrates that rectification of monovalent ion flow through the α HL channel can be related to the asymmetry in the location of the ionizable amino acid side chains.

Key words: Nernst-Planck analysis — Alpha hemolysin — Alpha toxin — Ion channel — Electrostatics

Introduction

Being able to predict the current-voltage relationship of ionic channels from first principles is still elusive, although significant progress towards that goal has been made in the last two decades (e.g., Jordan, 1982, 1983, 1984a,b, 1987; Cooper, Jakobsson & Wolynes, 1985; Levitt, 1985; Barcilon et al., 1993; Chen, Barcilon & Eisenberg, 1992; Chen & Eisenberg, 1993; Eisenberg, Klosek & Schuss, 1995; Chen, Lear & Eisenberg, 1997; Kurnikova et al., 1999; Miller, 1999; Cárdenas, Coalson & Kurnikova, 2000). Some of the difficulties arise because the structures of many channels are not known, the conformations of the channels may change with the magnitude and sign of the applied potential, and there are weaknesses as-

sociated with the various theoretical approaches. For example, a molecular dynamics approach using ion trajectories through the channel to determine the current can have limitations because of the rapid motions of atoms forming the channel and time requirements using today's computers (Nonner, Chen & Eisenberg, 1999; Levitt, 1999).

The *Staphylococcus aureus* α -hemolysin (α HL) channel might prove useful in testing modern physical theories of ionic conduction through nanoscale pores for several reasons. Much is already known about its ability to conduct ions (Menestrina, 1986; Bezrukov & Kasianowicz, 1993; Kasianowicz & Bezrukov, 1995), the crystal structure of the pore was recently determined (Song et al., 1996), and the pore can remain fully open indefinitely (Kasianowicz, 1994). Also, the crystal structure (Song et al., 1996), ionic conductance (Menestrina, 1986) and non-electrolyte polymer exclusion studies (Krasilnikov et al., 1992; Bezrukov et al., 1996; Korchev et al., 1995; Bezrukov & Kasianowicz, 1997, 2002; Krasilnikov, 2002) suggest that the limiting aperture of the channel's lumen is large relative to many other channels, including gramicidin (Russell et al., 1986; Koeppe, Mazet & Anderson, 1990; Becker et al., 1991).

The α HL protein is secreted by *Staphylococcus aureus* as a water-soluble monomer with a molecular mass of 3.3×10^4 grams/mole. These monomers bind spontaneously to lipid membranes and self-assemble into a heptameric channel (Gouaux, 1994; Song et al., 1996; Braha et al., 1997; Gouaux, 1998). Earlier, biochemical assays had suggested that after binding to detergent or membranes, α -hemolysin oligomerizes (Bhakdi, Fussle & Tranum-Jensen, 1981) into a hexamer (Tobkes et al., 1985), not a heptamer.

While it has been known that changing the charge state of ionizable residues in a channel can affect the channel's conductance (e.g., Prod'hom, Pietrobow & Hess, 1987; Bezrukov & Kasianowicz, 1993; Root & MacKinnon, 1994; Kasianowicz &

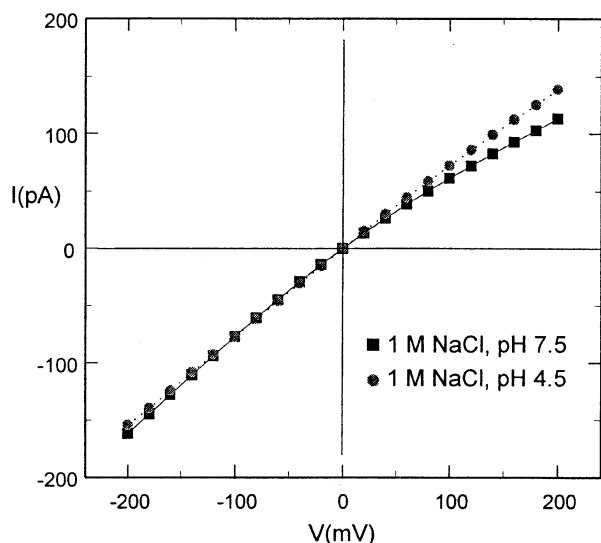


Fig. 1. A comparison of the I - V relationship for single *Staphylococcus aureus* α -hemolysin (α HL) channels in the presence of 1 M NaCl, pH 4.5 (circles) and pH 7.5 (squares).

Bezrukov, 1995; Rostovtseva et al., 2000), we demonstrate here the plausibility of the effect for the particular case of the α HL channel. The current-voltage relationship of this channel is, in general, nonlinear and rectifying and the nonlinearity is pH dependent (Fig. 1). In an effort to describe these characteristics, we use a highly simplified model that considers only the applied membrane potential and the Coulomb interactions between the permeant ions and the fixed charges associated with amino acids that line the channel's wall. Because the membrane is net neutral, fixed charges on the surface of the membrane are not considered (Lindemann, 1982; Krasilnikov & Sabirov, 1989). The model is based on a one-dimensional Nernst-Planck equation (Hille, 1992). It shows semi-quantitatively that some of the measured characteristics of the current-voltage (I - V) relationship at different pH values and different ionic concentrations can be explained by the Coulomb interactions. The approach, while simplified, may serve as a useful tool for researchers attempting to understand the conductive properties of relatively large channels that are not as well characterized as the α HL channel.

Materials and Methods

BILAYER FORMATION, SINGLE-CHANNEL RECONSTITUTION

The experimental chamber has been described earlier (Bezrukov & Kasianowicz, 1993) and is fabricated from polytetrafluoroethylene (PTFE). Partitions made of PTFE film 0.025 mm thick with hole diameters that varied from about 80 μ m to 100 μ m were used to divide the chamber in two halves and bilayer lipid membranes were

formed across the hole as described below. The lipid for forming the membrane, lyophilized 1,2-diphytanoyl-sn-Glycero-3-Phosphocholine (Avanti Polar Lipids, Alabaster, AL)¹ is mixed with pentane (10 mg/1 mL). The lipid bilayer is formed across the hole using a variation of a technique devised by Montal and Mueller (1972). Initially, NaCl solution partially fills each half of the chamber (volume: 2 mL; surface area: 0.97 cm²). Approximately 15 μ L of lipid is applied to the NaCl surfaces when the levels are just below the hole in the partition. The NaCl levels are slowly raised in sequence to a point just above the hole to form the lipid bilayer. The additional NaCl is introduced into the chamber via PTFE tubes connected between the chamber and syringes filled with NaCl, and the process is monitored visually by observing the NaCl levels through a microscope. During the raising of the NaCl levels, an ac voltage is applied across the partition and the creation of the membrane is signaled by a sudden step increase in the capacitively coupled current. Prior to raising the NaCl levels, the rim of the hole is coated with hexadecane using a solution of hexadecane in pentane (1:100 v/v).

Details of the experimental method for reconstituting the α HL ionic channel into the bilayer membrane are described elsewhere (Kasianowicz & Bezrukov, 1995; Kasianowicz et al., 1999). Briefly, following formation of the membrane, 0.4 μ L to 0.5 μ L of α HL is added to one half of the chamber (the *cis* compartment), while stirring, with an applied membrane potential of about plus or minus 60 mV. Ag/AgCl electrodes (In-Vivo Metrics, Healdsburg, CA) are used to apply the voltage across the PTFE partition and membrane. Creation of one or more ion channels is indicated when a dc signal proportional to the current is observed. During acquisition of current-voltage (I - V) data, the membrane potential, E , was applied to the *cis* end of the channel (the *trans* side is at ground potential) and varied in steps under computer control from -200 mV to 200 mV. All experiments were performed at room temperature, i.e., $22.5 \pm 1^\circ\text{C}$.

MODEL

We model the transport of monovalent ions through the α HL channel using the one-dimensional Nernst-Planck equation for current density, J_S , which, after integration can be expressed as (Hille, 1992)²

$$J_S = -z_S F \beta \frac{[S]_o - [S]_i \exp(v)}{\int_{x=0}^{x=l} [\exp(z_S F \psi(x)/RT)/D_S] dx} \quad (1)$$

where $v = z_S EF/RT$, z_S is the valence of ion species S , F/RT has its usual meaning, $[S]_i$ is the concentration of ion species S , for our arrangement, on the *cis* side of the channel, $[S]_o$ is the concentration of S on the *trans* side, l is the length of the channel (10.0 nm, [Song et al., 1996]), D_S is the diffusion coefficient for species S , β is the water-membrane partition coefficient for S , e.g., $\beta[S]_o$ is the ion concentration just inside the membrane at $x = l$, and $\psi(x)$ is the electrostatic potential profile inside the channel.

We make no attempt to determine $\psi(x)$ using a self-consistent approach such as solving Poisson's equation for an assumed charge distribution and boundary conditions in the channel, and superimposing the membrane potential applied across the membrane

¹The identification of commercial materials and their sources is made to adequately describe the experimental results. In no case does this identification imply recommendation by the National Institute of Standards and Technology, nor does it imply that the material is the best available.

²Correcting for a typographical error.

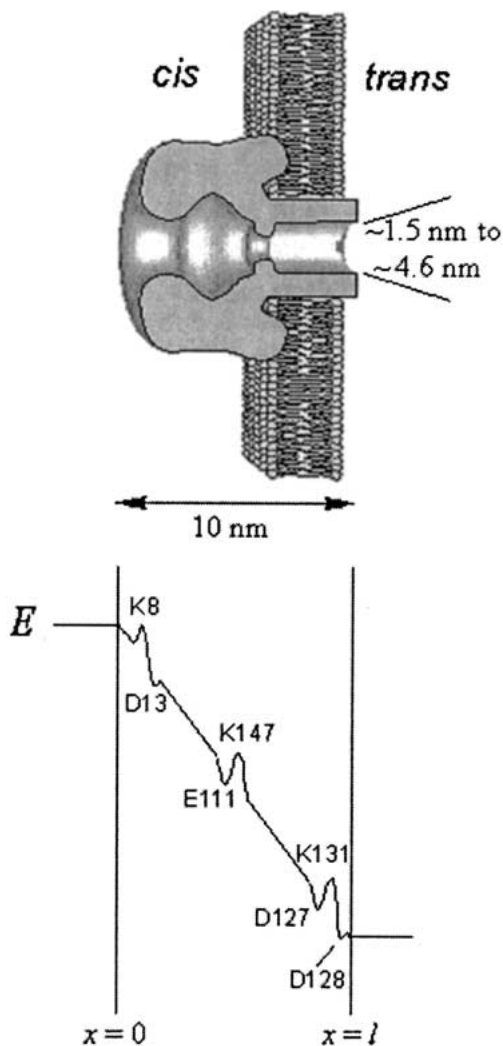


Fig. 2. A cartoon depiction of the α HL channel (top). A simplified electrostatic potential profile identifying the charged amino acid side chains that are inside the pore or close to the pore entrances (bottom). E is the applied potential.

and channel. Rather, to keep the model simple, we assume that the potential profile $\psi(x)$ within the α HL channel (Fig. 2, top) consists of barriers and wells superimposed on a linear applied potential, as is shown qualitatively in Fig. 2, bottom.³ The assumption of a linear potential (the constant field assumption), leads to the Goldman-Hodgkin-Katz equation that has been used elsewhere when modeling (in a simplified way) ion currents through channels (Hille, 1992). The barriers and wells are associated with specific charged amino acids found in the α HL channel. In our simplified model, the charges on the amino acid side chains form rings of charge. That is, for a given amino acid, one charged site can exist on each of the 7 monomers forming the α HL channel and is represented in a one-dimensional model as a barrier or well.

We note however, that the amplitude of the barriers and wells that are used to obtain reasonable fits of the I - V data are small compared to calculated values of the potential from a ring of charge in vacuum (e.g., $7e$) along its axis. Considerable field at-

tenuation is expected because the charged amino acid side chains are located near a surface of dielectric constant ~ 2 and face an electrolyte solution with static dielectric constant ~ 80 (e.g., approximately by a factor of 40 for a plane boundary) (Jackson, 1975; Aveyard & Haydon, 1973; McLaughlin, 1977, 1989; Jordan et al., 1989). In addition, we assume that the permeant ions are perhaps one or two Debye lengths away from the fixed-charge sites at their closest approach. Thus the ions encounter barriers and wells that have amplitudes of tens of millivolts, rather than volts. For our purposes, the precise amplitudes are not as important as how the I - V relationships are affected by changes in the amplitudes when the pH values of the electrolyte solutions are changed. The fits to the data discussed below are not unique. That is, fits to the data could be obtained with different sets of amplitudes and locations for the barriers and wells if locations other than those obtained from the crystal structure are used.

Other approximations are also made. For example, perturbations of the applied membrane potential by the channel's vestibule and constriction (Fig. 2, top) are ignored. Also ignored are variations in the radii of the charge rings, potentials due to charges induced by the mobile ions in the membrane and protein dielectric, image charges induced by the mobile ions in the membrane and protein dielectric (Jackson, 1975; McLaughlin, 1977; Jordan et al., 1989), and Coulomb interactions between the mobile ions. Although the relatively large inside diameter of the α HL channel (~ 1.5 nm to 4.6 nm compared to ~ 0.4 nm for gramicidin) may reduce the severity of these and other approximations noted herein, we readily acknowledge the considerable simplification of the problem.

Nevertheless, the calculated shapes of the I - V relationships from our model capture the essence of the I - V measurements at different pH values and ion concentrations, lending support to the view that ion/(charged) amino-acid interactions play a significant role controlling ion transport through the α HL channel. The approach used here cannot, because of its considerable simplicity, substitute for more comprehensive and rigorous treatments of the problem described (e.g., Barcilon et al., 1993; Eisenberg et al., 1995; Kuyucak, Hoyles & Chung, 1998) or discussed recently in the literature (Levitt, 1999; Nonner et al., 1999). Rather, by demonstrating the possible direct influence of charged sites within the channel on ion transport, the results may complement more careful model calculations.

The candidate amino acid side chains that we consider, their assumed (fixed) distances from the *cis* end of the channel, and their pK values (Voet & Voet, 1995) are listed in Table 1. The distances are taken from X-ray crystal structure coordinates (A. Cárdenas, private communication). The barriers and wells are assumed to have Gaussian potential profiles with the standard deviation, σ , treated as the effective Debye length. For our measurements, the bulk monovalent salt concentrations on the *cis* and *trans* side were equal, i.e., $[S]_i = [S]_o$. Assuming a constant diffusion coefficient in the channel, and multiplying and dividing the integrand in Eq. (1) by zFE/RTl , the expression for current density can be rewritten

$$J_S = -z^2 F \frac{E}{l} \beta u_s [S] \frac{1 - \exp(v)}{\int_{x=0}^{x=l} \frac{zFE}{RTl} [\exp(z_S F \psi(x)/RT)] dx}, \quad (2)$$

where the mobility of ion species S , u_s , is introduced, assuming its relation to the diffusion coefficient, $D = RTu_s/F$ is valid. We also assume that the ion mobilities for Na^+ ($5.19 \times 10^{-4} \text{ cm}^2/\text{Vs}$) and Cl^- ($7.92 \times 10^{-4} \text{ cm}^2/\text{Vs}$) in bulk media are valid inside the channel.

The potential profile in the channel is given by

$$\psi(x) = \frac{E}{l}(l-x) + \sum_i A_i \exp\left[-\frac{(x-x_{oi})^2}{\sigma^2}\right], \quad (3)$$

³The actual potential profiles will have different appearances because of the overlap between adjacent barriers and wells. See Fig. 5.

where the first term represents the applied membrane potential and A_i is the amplitude of the i^{th} well or barrier and x_{oi} is its position along the x -axis.

The integral in Eq. 2 is calculated numerically using Simpson's Rule. Because the one-dimensional Nernst-Planck approach does not include a method for determining *ab initio* the absolute ionic current through a channel, we normalized the calculated current density, J_S , to the measured current at one voltage (either +200 mV or -200 mV). This procedure is reasonable because a simple calculation for the ionic current through a uniform, right circular cylindrical pore with a 0.8 nm radius would yield ionic currents that are within a factor of three of the measured values.

Results and Discussion

TITRATION RESULTS AND DISCUSSION

Our measurements of the I - V relationship for single and multiple channels formed by the α HL toxin were performed using several concentrations of NaCl and two different pH values. Two channel types are typically observed with 1 M, 10 mM HEPES, pH 7.5 solutions. The I - V relationships for the two channel types were characterized by their current rectification ratios, γ_{120} , of ~ 1.3 and 1.6, where γ_{120} is defined as the ratio of ionic currents at -120 mV and +120 mV, i.e., $|I(-120 \text{ mV})/I(+120 \text{ mV})|$. We show here only the I - V data for the channel with the greater conductance and with $\gamma_{120} \sim 1.3$ (e.g., Fig. 1).

Three channel types were observed using 1 M NaCl, 10 mM citric acid, pH 4.5 and pH 4.55 solutions, but one channel type was observed most often with $\gamma_{120} \sim 1.08$. Beginning with this type of channel, several experiments were performed to determine if it corresponded to either of the channel types observed at pH 7.5. A titration of the *cis* and *trans* sides of the channel from pH ~ 4.5 to pH 7.2 showed that the channels formed at pH 4.5 ($\gamma_{120} \sim 1.08$) corresponded to the channel with $\gamma_{120} \sim 1.3$ (pH 7.5). That is, the I - V relationships for the titrated channel and the channel formed at pH 7.5 agreed (*see below*).

However, one focus of this paper is to describe how protons binding to different parts of the α HL channel affect the pore's I - V relationship. Specifically, we investigate the effects of sequentially titrating the pH value of the two bulk aqueous phases bathing the pore. We also show how changes to the ionic strength alter the channel's conducting properties. It is from these data and model calculations that we conclude that the I - V characteristics are controlled, to a large extent, by electrostatic interactions between the permeant ions and the charged amino-acid residues inside the pore or near the pore entrance.

Figure 3a illustrates the change in the single α HL channel I - V relationship before and after increasing the pH value on the *cis* side of the membrane (i.e., the side to which proton is added, *see Fig. 2*). The channel is first bathed by 1 M NaCl at pH 4.55 on

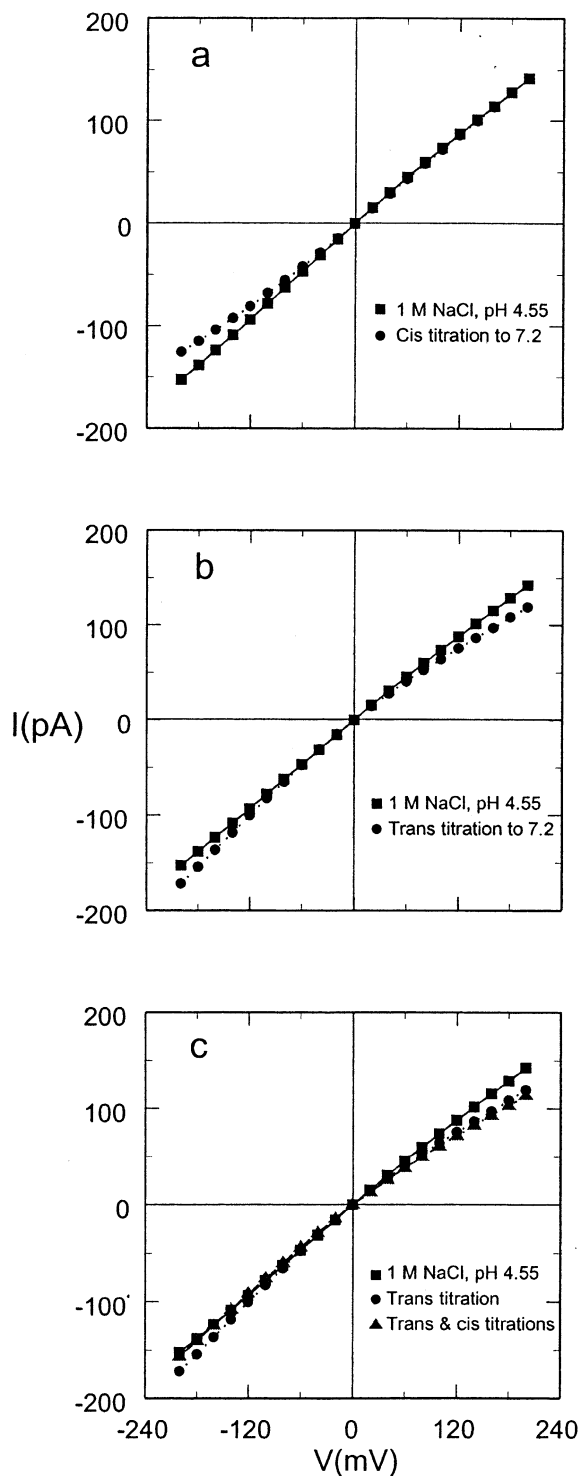


Fig. 3. Effect of partial and sequential pH changes on the I - V relationship for single *S. aureus* α HL channels. (a) I - V relationship before and after changing the pH in only the *cis* compartment from pH 4.5 to 7.2. (b) I - V relationship before and after changing the pH in only the *trans* compartment from pH 4.5 to 7.2. (c) I - V relationships for the sequential titrations of the pH value in the *trans* compartment followed by the *cis* compartment. Initially the solutions in both compartments contain 1 M NaCl (10 mM citric acid). The increase in pH is obtained by adding $\sim 120 \mu\text{L}$ of 0.5 M HEPES in 1 M NaCl (pH 7.5) to each compartment.

both sides of the membrane and the I - V relationship is slightly nonlinear. Adding ~ 120 μL of 0.5 M HE-PES in 1 M NaCl, pH 7.5 to the *cis* side raises the pH on that side of the membrane to 7.2. It is interesting that while there is no significant change in current for positive membrane potentials, there is a marked reduction in the channel's conductance for negative applied membrane potentials.

The corresponding results for a single channel with the pH titration performed only on the *trans* side, is shown in Fig. 3*b*. For this case, there is a decrease in current for positive membrane potentials. However, there is also an increase in the current for large negative membrane potentials.

Figure 3*c* shows the I - V relationships when the pH titrations are performed in sequence, i.e., a *trans* titration followed by a *cis* titration. The I - V relationship following the sequential titration is nonlinear and rectifying, which is in good agreement with the I - V data recorded for single channels formed in the presence of 1 M NaCl, pH 7.5 on both sides of the membrane (Fig. 1). When the pH titrations are performed in the reverse order (i.e., *cis* then *trans*, *data not shown*), the final I - V relationship is virtually indistinguishable from the results shown in Fig. 3*c* (*filled triangles*).

The effects of changing the pH on the αHL channel's I - V relationship cannot be ascribed to the current of protons (i.e., H_3O^+) flowing through the pore for several reasons. First, the pore is relatively large and only weakly ion-selective. Second, the concentration of protons is much less than that of Na^+ and Cl^- . Third, the titration of the pH to greater values on the *trans* side causes the current to increase in one quadrant of the I - V relationship and decrease on the other. The results in Fig. 3 also suggest that there are ionizable amino acid side chains adjacent to or near both channel entrances. This point is discussed below.

We interpret the experimental results using the one-dimensional Nernst-Planck model described in the Materials and Methods section. Figure 4 reproduces the data shown in Fig. 3*c* and the corresponding results of the model calculations. To model the I - V data at pH ~ 4.5 (Fig. 4*a*), we assume that the amino acid side chains have the same pK that they would have in an infinitely dilute bulk solution. That is, the amount of negative charge contributed by amino acids D13, E111, D127, and D128 is less than that from the fully positively charged amino acids K8, K147, and K131 because of their respective pK values (Table 1). Consistent with this assumption, we assign amplitudes to the barriers and wells that lead to a good fit (Fig. 4*a*, *empty squares*) of the model to the data. Specifically, the barrier and well amplitudes (A_i in Eq. 3) are 26 mV, -11 mV, -11 mV, 26 mV, -11 mV, 26 mV, and -11 mV for K8, D13, E111, K147, D127, K131, and D128, respectively, at the

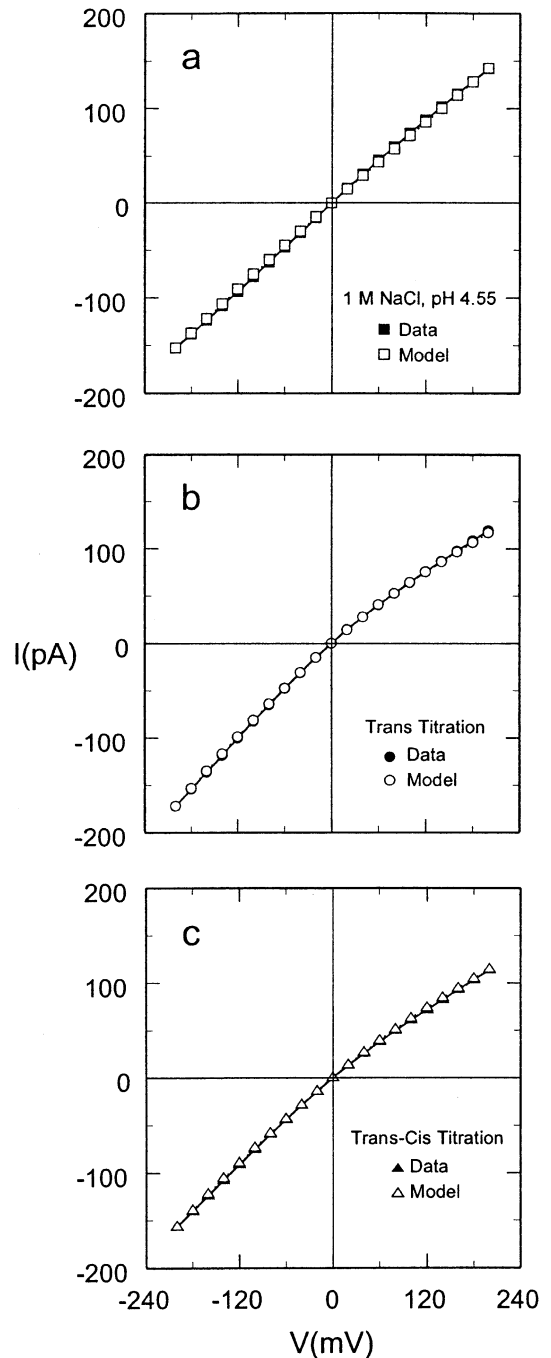


Fig. 4. Comparison of experimental results with model predictions. (a) pH 4.5 both compartments. (b) $\text{pH}_{\text{cis}} = 4.5$, $\text{pH}_{\text{trans}} = 7.2$. (c) pH 7.2, both compartments. The solutions contained 1 M NaCl. The calculated current density was normalized to the current value at -200 mV (a, b and c). See text for details.

locations indicated in Table 1. In our highly simplified model, the value of σ , the effective Debye length, is assumed to be 0.3 nm, i.e., the Debye length for a planar surface containing fixed charges in the presence of a 1 M 1:1 electrolyte solution [McLaughlin, 1977] and the calculated current density is normalized to the current value at -200 mV.

Table 1. Candidate amino-acid information for model

Amino acid	Distance from <i>cis</i> entrance (nm)	pK value
Lys ⁸ (K8)	1.13	10.5
Asp ¹³ (D13)	1.84	3.9
Glu ¹¹¹ (E111)	5.06	4.1
Lys ¹⁴⁷ (K147)	5.10	10.5
Asp ¹²⁷ (D127)	9.82	3.9
Lys ¹³¹ (K131)	9.85	10.5
Asp ¹²⁸ (D128)	9.95	3.9

In assigning the barrier and well amplitudes to obtain the good fit of the data, we have ignored what their relative amplitudes should be according to the Henderson-Hasselbach relationship and the pK values of the amino acids. However, the lower amplitudes of the wells are expected because the bulk pH is close to their pK values.

For the *trans*-side titration of the pH from ~ 4.5 to 7.2, the single-channel current decreases for positive applied potentials and increases for negative potentials (Fig. 3b). If the channel's geometric structure is unaltered by the change in pH, the decrease in the total ionic current could either be caused by a decrease in the flow of negative ions from *trans* to *cis*, positive ions from *cis* to *trans*, or both. Because the pH was altered only on the *trans* side, we assume that the negative ionic current decreases from that side because the negative charge density of the amino acid side chains near the *trans* entrance increases. The carboxylic acid side chains that are closest to the *trans* entrance are D127 and D128 (Table 1 and Fig. 2, *bottom*) and will be most strongly affected. In addition, for positive applied potentials, the positive ion current that flows from *cis* to *trans* will remain virtually unchanged for a change in the pH value on the *trans* side because the potential well depth associated with D13 near the *cis* entrance is assumed to not change significantly.

Reasoning in a similar manner, the likely cause of the increase in total ionic current for negative applied potentials is due to the increase of positive ionic flow from *trans* to *cis*, because of the increase in negative charge from D127 and D128 near the *trans* entrance.

We assume that the effect of the *trans*-side pH titration on other ionizable amino acids becomes negligible as their distance from the *trans* entrance increases and we assign potential barrier amplitudes (A_i in Eq. 3) that are consistent with this assumption. The potential barrier amplitudes for the lysines that line the channel lumen are expected to remain unchanged because of their relatively high pK value (Table 1).

Taking into account the above expected trends in barrier and well amplitudes, a good fit of the I - V relationship for a *trans*-only pH titration was obtained (Fig. 4b, *empty circles*) by assuming ampli-

tudes $A_i = 26$ mV, -11 mV, -11 mV, 26 mV, -26 mV, 26 mV, and -26 mV for K8, D13, E111, K147, D127, K131, and D128, respectively. The amplitude adjustments are for D127 ($\Delta = -15$ mV) and D128 ($\Delta = -15$ mV); no changes are made for K8, D13, E111 and K147. The well amplitudes near the *trans* end of the channel now correspond to fully charged negative rings. The value of σ is assumed to be 0.3 nm and the calculated current density is normalized to the current value at -200 mV.

To model the I - V relationship for subsequently increasing the *cis* pH value from ~ 4.5 to 7.2, we note that the total current decreases for negative membrane potentials and decreases slightly for positive membrane potentials (Fig. 3c). For negative applied potentials, the reduction in total current can be explained by an increase in the amplitude of the well for negative ions near the *cis* end of the channel (D13) and to a lesser extent by the well associated with E111 (Fig. 2, *bottom*) that occurs when the pH is increased further above their pK values.

The slight decrease in total ionic current for positive membrane potentials is somewhat difficult to explain in full, but not unexpected. Beginning with pH ~ 4.5 salt solutions in both compartments, the *cis*-only titration data does show a slight decrease in current for most positive voltages, e.g., 1.3% at 120 mV in Fig. 3a. Small attenuation of the total current would occur when the well amplitude associated with E111 is increased because (if acting alone) it is a barrier for negative ions regardless of membrane potential. It also enhances positive ionic current, but because of the greater mobility and numbers of the negative ions, the net result is a loss of total current. The actual modeling is more complicated, however, because when the *cis* titration is performed, the well amplitude for D13 also increases. In addition, the E111 well and K147 barrier are in close proximity and as shown below, the two cancel each other to a great extent.

Assuming that the subsequent *cis* titration increases the amplitudes of the wells associated with D13 and E111 to their fully charged state (-26 mV), the calculated I - V relationship (*empty triangles*, Fig. 4c) is in good agreement with the measured results (*filled triangles*). That is, the amplitudes of the barriers and wells for pH 7.2 are 26 mV, -26 mV, -26 mV, 26 mV, -26 mV, 26 mV, and -26 mV for K8, D13, E111, K147, D127, K131, and D128, respectively. The calculated current density in Fig. 4c is normalized to the current value at -200 mV.

As noted earlier, when the pH titrations are performed in reverse order (*cis* followed by *trans*), the final I - V relationship at pH 7.2 agrees with the results in Fig. 3c. To be consistent with the *trans*-*cis* sequential model calculation, the corresponding calculation for the *cis*-only titration requires that the well amplitudes for D13 and E111 be increased to -26

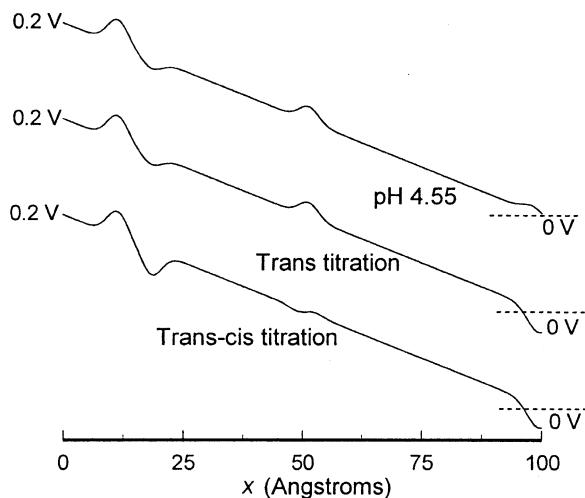


Fig. 5. Potential profiles used for the model calculations in Fig. 4 with pH 4.5 both compartments, $\text{pH}_{\text{cis}} = 4.5$, $\text{pH}_{\text{trans}} = 7.2$, and pH 7.2, both compartments. An applied potential of +200 mV is assumed for the profiles shown here.

mV and that the well amplitudes for D127 and D131 remain at -11 mV. The results of this calculation (*not shown*) indicate good agreement with the data (Fig. 3a) between -100 mV and $+200$ mV when the calculated current density is normalized to the current at $+200$ mV, the membrane potential for which the current is unaffected by the pH change. However, below -100 mV, the model underestimates the decrease in current. At -200 mV, the current data shows a decrease of 18% with respect to the current at pH 4.55 (Fig. 3a), whereas the model predicts an 8% decrease. The discrepancy is no doubt attributable to the simplicity of our model.

Figure 5 illustrates the actual potential profiles used to calculate the shapes of the I - V relationships for pH 4.5 on both sides, after changing the pH in the *trans* compartment (*trans* titration) and after changing the solution pH values in both compartments (*trans-cis* titration). An applied potential of $+200$ mV is assumed in the figure. The appearances of the profiles differ significantly from the simplified depiction in Fig. 2 (*bottom*) because of the overlap of the wells and barriers. Although the electric field from the side chain at D128 extends into the bulk aqueous phase, contributions to the integral in Eq. 1 from outside the channel are ignored.

We assumed above that changing the pH of the solution near the *trans* (*cis*) end of the channel would not have a substantial effect on the barrier and well amplitudes of ionizable amino acid side chains adjacent to the *cis* (*trans*) end of the α HL channel, and thus on the current originating from the *cis* (*trans*) side of the channel. Predictions for the I - V relationship (Eq. 2) are consistent with this effect on the ionic current. For example, using the amplitude adjustments for fitting the *trans* pH titration data (Fig. 4b),

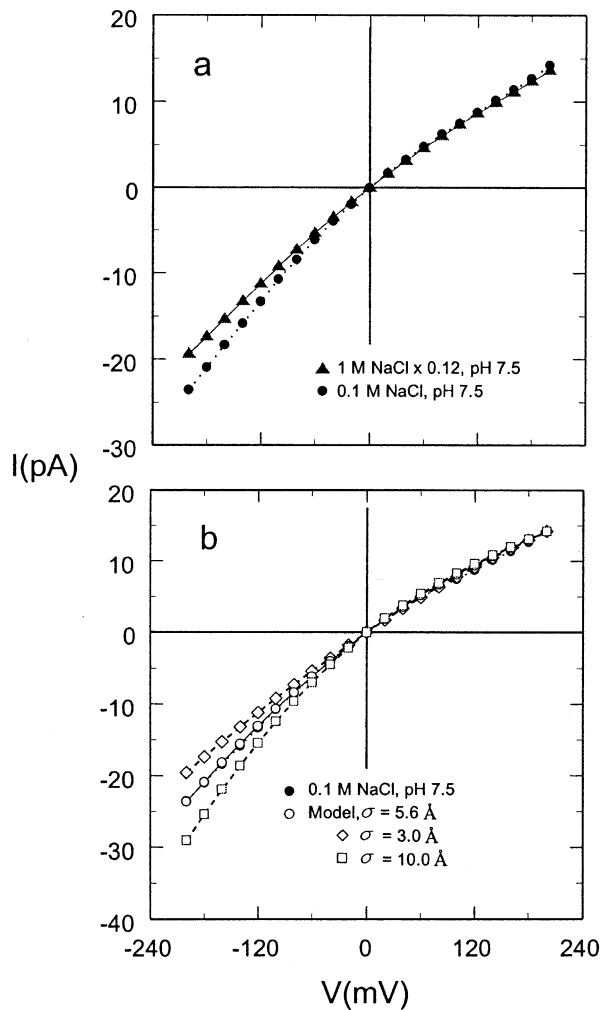


Fig. 6. I - V relationships for single α HL channels in 1 M NaCl and 0.1 M NaCl, pH 7.5. (a) For comparison, the data obtained in the presence of 1 M NaCl data was multiplied by 0.12 to adjust for differences in the measured bulk conductivities of the salt solutions. (b) Results of model calculations for fitting to the experimental data with 0.1 M NaCl shown in (a) with an effective Debye length of 5.6 Å (circles). Comparisons are given for calculated current values assuming effective Debye lengths of 3 Å (diamonds) and 10 Å (squares). The calculated currents are normalized to the current value at $+200$ mV.

the calculated current densities originating from the *cis* end of the channel were unchanged at the extremes of membrane potentials (± 200 mV).

ALTERING THE IONIC CONCENTRATION

For fixed pH values, changing the NaCl concentration allows us to evaluate how other parameters (e.g., the effective Debye length) modify the I - V relationship. We investigated this possibility by comparing the I - V data obtained with 1 M, 0.3 M and 0.1 M NaCl solutions, and performed model calculations starting with a potential profile that resulted in good fits with the higher molarity data.

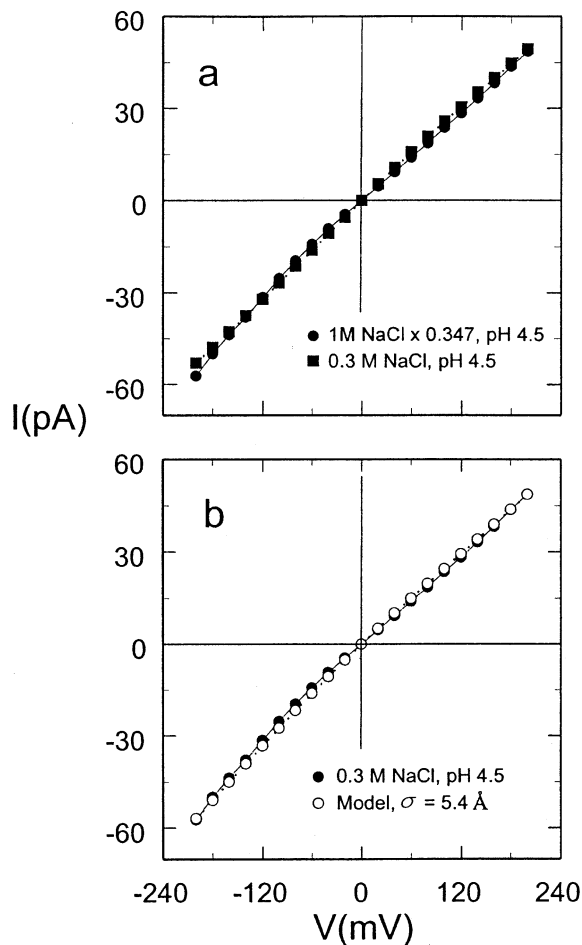


Fig. 7. I - V relationships for single α HL channels in 1 M NaCl and 0.3 M NaCl, pH 4.5. (a) The 1 M data was multiplied by 0.347 to adjust for differences in the measured conductivities of the salt solutions. (b) Results of model calculation for fitting to the 0.3 M experimental data shown in (a) with the indicated effective Debye length. The calculated current density is normalized to the current value at +200 mV.

Measurements of the single- α HL-channel I - V relationships at 0.3 M NaCl and 0.1 M NaCl (both at pH 7.5) were recorded and compared to the I - V data obtained with 1 M NaCl (pH 7.5). As stated above, two channel types with rectification ratios γ_{120} of ~ 1.3 and 1.6 were observed for 1 M NaCl. To compare the I - V relationship obtained with channels formed in 1 M and 0.1 M NaCl solutions, we scaled the 1 M data by the ratio of the measured bulk conductivities. A correspondence was identified between the channel formed in the presence of 1 M NaCl ($\gamma_{120} \sim 1.3$) and that formed in 0.1 M NaCl, as is shown in Fig. 6a.

Figure 6b shows the fit of the model (*empty circles*) to the 0.1 M NaCl I - V data by normalizing the calculated current density to the current value at +200 mV. The potential profile, i.e., the barrier and well amplitudes, are the same as those used for fitting

the 1 M NaCl data (Fig. 4c, *triangles*), but the value of the effective Debye length is increased from 0.3 nm (1 M NaCl) to 0.56 nm (0.1 M NaCl). Similar data obtained in the presence of 0.3 M NaCl are described by an effective Debye length of 0.42 nm (*data not shown*). The increase in the effective Debye-length values deduced from fitting Eq. 2 to the data in the presence of 0.3 M and 0.1 M NaCl are less than expected from a simple theoretical calculation for the ionic atmosphere surrounding an isolated fixed charge (Aveyard & Haydon, 1973; McLaughlin, 1977; Hille, 1992). Nevertheless, it is noteworthy that the shape of the calculated I - V relationship could be made to match the data simply by increasing the effective Debye length (Eq. 3). For comparison, Fig. 6b also shows poorer calculated fits to the data, assuming Debye lengths of 3 Å (*empty diamonds*) and 10 Å (*empty squares*). All of the calculated results are normalized to the current value at +200 mV because the change in ionic concentration has little effect on the current for this membrane potential (Fig. 6a).

We repeated the experiments for single channels formed at pH 4.5. Two channel types with rectification ratios of $\gamma_{120} \sim 0.89$ and 1.11 were observed when the channels were formed in the presence of 0.3 M NaCl (because channels formed in 0.1 M NaCl tend to gate excessively, their I - V measurements are not reported here). After correcting for the different measured bulk conductivities, the channel with $\gamma_{120} \sim 1.11$ in 0.3 M NaCl corresponded with the channel formed at 1 M (Fig. 7a).

Figure 7b shows the fit of Eq. 2 to the 0.3 M data by normalizing the calculated current density to the current value at 200 mV. The potential profile used for modeling the shape of the I - V relationship for the α HL channel in 0.3 M NaCl (pH 4.5) is the same as for the 1 M NaCl data (Fig. 4a), except that the effective Debye length has been increased from 0.3 nm to 0.54 nm.

The increase in the effective Debye length that accompanies the decrease in the ionic strength is reassuring. However, that one cannot take these estimates too seriously is underscored by the difference in the effective Debye length with pH. For example, the estimated values for σ , from the model calculations, are 0.42 nm and 0.54 nm for 0.3 M NaCl solutions at pH 7.5 and pH 4.5, respectively.

Conclusions

The purpose of this study was to show that the control of ionic current flow through the α HL channel is primarily electrostatic in nature. A one-dimensional Nernst-Planck model (Hille, 1992) coupled with the positions of the charged amino acids in or near the α HL channel lumen indicated by the channel's crystal structure (Song et al., 1996) captures

the essence of the experimental data shown here. Although there are many assumptions implicit in this simple approach, our goal here is to show that direct Coulomb interactions occur between specific fixed charges and the permeant ions. This information will be useful to theorists who perform more detailed and realistic calculations. The highly simplified approach that we have used could also help investigators understand the conductive properties of channels that have unknown structures.

As noted earlier, the I - V relationship of a single α HL ion channel is nonlinear and rectifying (Fig. 3). An early simple analytical study by Neumcke showed that electrostatics could account for rectification in the I - V relationship for ionic flow through membranes. In particular, strong rectification occurs if the charges on the two membrane surfaces are opposite in sign (Neumcke, 1970). Subsequent experimental studies on a K^+ channel (Bell & Miller, 1984) and on the α HL channel (Krasilnikov & Sabirov, 1989) showed that the charge on the surface of a membrane could alter channel I - V relationships.

Because fixed charges on a membrane surface can alter the conductance of a membrane or an ion channel, it follows that fixed charges inside a channel lumen, and/or in the channel near the pore entrances, should alter either the channel conductance or gating properties (Levadny, et al., 2002). It was shown earlier that protons alter the conductance of channels (e.g., Prod'homme et al. 1987; Root & MacKinnon, 1994), including α HL (Bezrukov & Kasianowicz, 1993, 1997; Kasianowicz & Bezrukov, 1995). The conductance changes could be the result of either proton-induced conformation changes or perturbations of the transmembrane electrostatic potential profile, or both. The results in this paper suggest that, in the case of the α HL channel, the changes in the I - V relationship that occur following a change in the bulk pH can be ascribed to changes in the relative number of fixed charges in or near the channel's lumen. Although we cannot completely rule out the possibility of structural changes in the pore caused by protons binding to amino acid side chains, it is unnecessary to consider such changes in order to obtain good fits to the I - V data.

We also demonstrate that the rectification of monovalent ion flow through the α HL channel (Fig. 3) is related to the asymmetry in the location of ionizable amino acid side chains (Song et al., 1996). It was recently shown that negatively charged polynucleotides can be driven electrophoretically into and through single α HL channels (Kasianowicz et al., 1996). It was subsequently shown that at constant applied potential, the polynucleotides are more likely to enter the pore from the *cis* side than from the *trans* side at pH 7.5 (Henrickson et al., 2000). In that study, we speculated that the asymmetry in the partitioning of single-stranded DNA

into this channel might be caused either by the different radii of the two pore entrances (i.e., an entropy-dominated energy barrier) or by the difference in the electrostatic potential caused by the fixed charges in or near the channel's entrances. Because of the greater amount of negative charge near the *trans* pore mouth (Fig. 5, negative barriers following *trans* titration) it is likely that electrostatics alone could account for the asymmetric partitioning of polynucleotides into this channel.

This work was performed in part with the support from the NIST Advanced Technology Program, and the NIST "Single Molecule Manipulation and Measurement" program.

References

- Aveyard, R., Haydon, D.A. 1973. Principles of Surface Chemistry. Cambridge University Press, NY, NY
- Barcilon, V., Chen, D., Eisenberg, R.S., Ratner, M.A. 1993. Barrier crossing with concentration boundary conditions in biological channels and chemical reactions. *J. Chem. Phys.* **98**:1193-1212
- Becker, M.D., Greathouse, D.V., Koeppe, R.E. II, Anderson, O.S. 1991. Amino-acid sequence modulation of gramicidin channel function: effects of tryptophan-to-phenylalanine substitutions on the single channel conductance and duration. *Biochemistry* **30**:8830-8839
- Bell, J.E., Miller, C. 1984. Effects of phospholipid surface charge on ion conduction in the K^+ channel of sarcoplasmic reticulum. *Biophys. J.* **45**:279-287
- Bezrukov, S.M., Kasianowicz, J.J. 1993. Current noise reveals protonation kinetics and number of ionizable sites in an open protein ion channel. *Phys. Rev. Lett.* **70**:2352-2355
- Bezrukov, S.M., Kasianowicz, J.J. 1997. Charge state of an ion channel controls neutral polymer entry into its pore. *Eur. Biophysics J.* **6**:471-476
- Bezrukov, S.M., Vodyanov, I., Brutyan, R., Kasianowicz, J.J. 1996. Dynamics and free energy of polymer partitioning into a nanoscale pore. *Macromolecules* **29**:8517-8522
- Bezrukov, S.M., Kasianowicz, J.J. 2002. Dynamic partitioning of neutral polymers into a single ion channel. In: Structure and Dynamics of Confined Polymers. NATO Advanced Research Workshop. Eds. J.J. Kasianowicz, M. Kellermayer and D.W. Deamer. pp. 117-130. Kluwer Press, Dordrecht, The Netherlands
- Bhakdi, S., Fussle, R., Tranum-Jensen, J. 1981. Staphylococcal α -toxin, Oligomerization of hydrophilic monomers to form amphiphilic hexamers induced through contact with deoxycholate detergent micelles. *Proc. Natl. Acad. Sci. USA* **78**:5475-5479
- Braha, O., Walker, B., Cheley, S., Kasianowicz, J.J., Hobaugh, M.R., Song, L., Gouaux, J.E., Bayley, H. 1997. Structure-based design of a heteromeric transmembrane pore. *Chemistry & Biology* **4**:497-505
- Cárdenas, A.E., Coalson, R.D., Kurnikova, M.G. 2000. Three-dimensional Poisson-Nernst-Planck theory studies: Influence of membrane electrostatics on gramicidin A channel conductance. *Biophys. J.* **79**:80-93
- Chen, D.-P., Barcilon, V., Eisenberg, R.S. 1992. Constant fields and constant gradients in open ionic channels. *Biophys. J.* **61**:1372-1393
- Chen, D.-P., Eisenberg, R.S. 1993. Charges, currents, and potentials in ionic channels of one conformation. *Biophys. J.* **64**:1405-1421

- Chen, D.-P., Lear, J., Eisenberg, R.S. 1997. Permeation through an open channel: Poisson-Nernst-Planck theory of synthetic ion channel. *Biophys. J.* **72**:97–116
- Cooper, K., Jakobsson, E., Wolynes, P. 1985. The theory of ion transport through membrane channels. *Prog. Biophys. Molec. Biol.* **46**:51–96
- Eisenberg, R.S. 1996. Computing the fields in proteins and channels. *J Membrane Biol.* **150**:1–25
- Eisenberg, R.S., Klosek, M.M., Schuss, Z.E. 1995. Diffusion as a chemical reaction: Stochastic trajectories between fixed concentrations. *J. Chem. Phys.* **102**:1767–1780
- Gouaux, J.E., Braha, O., Hobaugh, M.R., Song, L.Z., Cheley, S., Shustak, C., Bayley, H. 1994. Subunit stoichiometry of Staphylococcal alpha-hemolysin in crystals and on membranes—a heptameric transmembrane pore. *Proc. Natl. Acad. Sci. USA* **91**:12828–12831
- Gouaux, E. 1998. α -Hemolysin from *Staphylococcus aureus*: An archetype of β -barrel, channel-forming toxins. *J. Structural Biol.* **121**:110–122
- Henrickson, S.E., Misakian, M., Robertson, B., Kasianowicz, J.J. 2000. Driven asymmetric DNA transport in a nanometer-scale pore. *Phys. Rev. Lett.* **85**:3057–3060
- Hille, B. 1992. Ionic channels of excitable membranes, 2nd ed. Sinauer Associates, Sunderland, MA
- Jackson, J.D. 1975. Classical Electrodynamics. J. Wiley & Sons, New York, NY
- Jordan, P.C. 1982. Electrostatic modeling of ion pores. Energy barriers and electric field profiles. *Biophys. J.* **39**:157–164
- Jordan, P.C. 1983. Electrostatic modeling of ion pores. II. Effects attributable to the membrane dipole potential profile. *Biophys. J.* **41**:189–195
- Jordan, P.C. 1984a. Effect of pore structure on energy barriers and applied voltage profiles. I. Symmetrical channels. *Biophys. J.* **45**:1091–1100
- Jordan, P.C. 1984b. Effect of pore structure on energy barriers and applied voltage profiles. II. Unsymmetrical channels. *Biophys. J.* **45**:1101–1107
- Jordan, P.C. 1987. Microscopic approaches to ion transport through transmembrane channels. The model system gramicidin. *J. Phys. Chem.* **91**:6582–6591
- Jordan, P.C., Bacquet, R.J., McCammon, J.A., Tran, P. 1989. How electrolyte shielding influences the electrical potential in transmembrane ion channels. *Biophys. J.* **55**:1041–1052
- Kasianowicz, J.J. 1994. Voltage-dependent gating kinetics of an ion channel modulated by ionic strength. *Biophys. J.* **66**:A430
- Kasianowicz, J.J., Burden, D.L., Han, L., Cheley, S., Bayley, H. 1999. Genetically engineered metal ion binding sites on the outside of a channel's transmembrane β -barrel. *Biophys. J.* **76**:837–845
- Kasianowicz, J.J., Bezrukov, S.M. 1995. Protonation dynamics of the α -toxin ion channel from spectral analysis of pH dependent current fluctuations. *Biophys. J.* **69**:94–105
- Kasianowicz, J.J., Brandin, E., Branton, D., Deamer, D.W. 1996. Characterization of individual polynucleotide molecules using a membrane channel. *Proc. Natl. Acad. Sci. USA* **93**:13770–13773
- Koeppel, R.E., Mazet, J.-L., Anderson, O.S. 1990. Distinction between dipolar and inductive effects in modulating the conductance of gramicidin channels. *Biochemistry* **29**:512–520
- Korchev, Y.E., Bashford, C.L., Alder, G.M., Kasianowicz, J.J., Pasternak, C.A. 1995. Low conductance states of a single channel are not 'closed.' *J Membrane Biol.* **147**:233–239
- Krasilnikov, O.V. 2002. Sizing channels with neutral polymers. In: Structure and Dynamics of Confined Polymers. NATO Advanced Research Workshop Eds. J.J. Kasianowicz, M. Kellermayer and D.W. Deamer. pp. 97–115. Kluwer Press, Dordrecht, The Netherlands
- Krasilnikov, O.V., Sabirov, R.Z. 1989. Ion transport through channels formed in lipid bilayers by *Staphylococcus aureus* alpha-toxin. *Gen. Physiol. Biophys.* **8**:213–222
- Krasilnikov, O.V., Sabirov, R.Z., Ternovsky, V.I., Merzliak, P.G., Muratkodjaev, J.N. 1992. A simple method for the determination of the pore radius of ion channels in planar bilayer membranes. *FEMS Microbiol. Immun.* **105**:93–100
- Kurnikova, M.G., Coalson, R.D., Graf, P., Nitzan, A. 1999. A lattice relaxation algorithm for three-dimensional Poisson-Nernst-Planck theory with application to ion transport through the gramicidin A channel. *Biophys. J.* **76**:642–656
- Kuyucak, S., Hoyles, M., Chung, S.-H. 1998. Analytical solutions of Poisson's equation for realistic geometrical shapes of membrane ion channels. *Biophys. J.* **74**:22–36
- Levadny, V., Colombini, M., Li, X.X., Aguilera, V.M. 2002. Electrostatics explains the shift in VDAC gating with salt activity gradient. *Biophys. J.* **82**:1773–1783
- Levitt, D.G. 1985. Strong electrolyte continuum theory solution for equilibrium profiles, diffusion limitation, and conductance in charged ion channels. *Biophys. J.* **48**:19–31
- Levitt, D.G. 1999. Modeling ion channels. *J. Gen. Physiol.* **113**:789–794
- Lindemann, B. 1982. Dependence of ion flow through channels on the density of fixed charges at the channel opening. *Biophys. J.* **39**:15–22
- McLaughlin, S.G.A. 1977. Electrostatic potentials at membrane-solution interfaces. *Curr. Topics Membrane Transport* **9**:71–144
- McLaughlin, S. 1989. The electrostatic properties of membranes. *Annu. Rev. Biophys. Chem.* **18**:113–136
- Menestrina, G. 1986. Ionic channels formed by *Staphylococcus aureus* alpha-toxin: Voltage-dependent inhibition by divalent and trivalent cations. *J. Membrane Biology* **90**:177–190
- Miller, C. 1999. Ionic hopping defended. *J. Gen. Physiol.* **113**:783–787
- Montal, M., Mueller, P. 1972. Formation of bimolecular membranes from lipid monolayers and a study of their electrical properties. *Proc. Natl. Acad. Sci. USA* **69**:3561–3566
- Neumcke, B. 1970. Ion flux across lipid bilayer membranes with charged surfaces. *Biophysik* **6**:231–240
- Nonner, W., Chen, D.P., Eisenberg, R.S. 1999. Progress and prospects in permeation. *J. Gen. Physiol.* **113**:773–782
- Prod'homme, B., Pietrobon, D., Hess, P. 1987. Direct measurements of proton transfer rates to a group controlling the dihydropyridine-sensitive Ca^{2+} channel. *Nature* **329**:243–246
- Root, M.J., MacKinnon, R. 1994. Two identical noninteracting sites in an ion channel revealed by proton transfer. *Science* **265**:1852–1856
- Rostovtseva, T.K., Liu, T.-T., Colombini, M., Parsegian, V.A., Bezrukov, S.M. Positive cooperativity without domains or subunits in monomeric membrane channel. 2000. *Proc. Natl. Acad. Sci. USA* **97**:7819–7822
- Russell, E.W.B., Weiss, L.B., Navetta, F.I., Koeppel, R.E. II, Anderson, O.S. 1986. Single channel studies on linear gramicidins with altered amino acid side chains. *Biophys. J.* **49**:673–686
- Song, L.Z., Hobaugh, M.R., Shustak, C., Cheley, S., Bayley, H., Gouaux, J.E. 1996. Structure of Staphylococcal alpha-hemolysin, heptameric transmembrane pore. *Science* **274**:1859–1866
- Tobkes, N., Wallace, B.A., Bayley, H. 1985. Secondary structure and assembly mechanism of an oligomeric channel protein. *Biochemistry* **24**:2192–2198
- Voet, D., Voet, J.G. 1995. Biochemistry. 2nd Ed. John Wiley & Sons, Inc., New York, NY